Response to Reviewer's comments

All responses and revisions in the revised manuscript are identified in **blue** text color.

Reviewer#2's comments:

This study is interesting and novel. It does provide a new perspective towards sulfate source apportionment, accounting for newer pathways for sulfate formation. I suggest the authors to comment on the following and make necessary changes in the manuscript:

1. Role of primary sulfates: I think this aspect has been overlooked. It needs to be quantified as the works of Daie et al. (2019) and Song et al., (2024) reveal nearly half of atmospheric sulfate could be attributed to primary sulfate. Once the authors attribute this fraction, the remaining can be attributed to secondary and as such Fig. 6 needs to show this division clearly with a separate sub-figure.

Response: We thank the reviewer for the insightful comment. In the revised manuscript, we have thoroughly refined the seasonal and process-specific partitioning of primary and secondary sulfates. To address the well-known underestimation of primary sulfate emissions, a factor that partially accounts for the missing sulfate phenomenon often encountered in chemical transport modeling, our refined mass-balance framework parameterizes anthropogenic primary sulfate (n_{ap}) as 3% of total anthropogenic sulfur emissions. Under the reasonable assumption that ambient SO_2 and secondary sulfate precursors are predominantly of anthropogenic origin, the molar concentrations of the various sulfate fractions are resolved through a coupled system of equations:

$$n_{ps} = n_{ss} + n_{ts} + n_{ap} \tag{1}$$

$$n_{ap} = 3\% \times \left(n_{SO_2} + n_{sas}\right) \tag{2}$$

$$n_{sas} = n_{tos} - n_{ss} - n_{ts} - n_{ap} \tag{3}$$

where n_{tos}, n_{ps}, and n_{sas} represent the molar concentrations of total, primary, and secondary atmospheric sulfate, respectively, with the primary fraction further resolved into sea-salt (n_{ss}), terrestrial (n_{ts}), and anthropogenic primary (n_{ap})

components. To constrain these natural backgrounds, we employed companion tracer concentrations and mass ratios; specifically, sea-salt sulfate was quantified from soluble Na^+ assuming a purely marine origin (n_{ss} =k[Na^+], where k=[SO_4^{2-}]/[Na^+]=0.25), while terrestrial sulfate was evaluated based on crustal Ca^{2+} abundances (0.18×[Ca^{2+}]). Building upon this physical allocation, the stable sulfur isotope signatures ($\delta^{34}S$) are integrated via an isotopic mass-balance framework to isolate the secondary formation pathways:

$$\delta^{34}S_{obs} = f_{ss} \times \delta^{34}S_{ss} + f_{ts} \times \delta^{34}S_{ts} + f_{ap} \times \delta^{34}S_{ap} + f_{sas} \times \delta^{34}S_{sas} \quad (4)$$

$$f_{ps} = f_{ss} + f_{ts} + f_{ap} \quad (5)$$

Here, $\delta^{34}S_{obs}$ denotes the bulk observed $\delta^{34}S\text{-}SO_4^{2-}$ value, while the terms prefixed with *f* represent the corresponding molar fractions of each discrete source relative to the total sulfate burden, matched with their respective endmember isotopic signatures ($\delta^{34}S_{ss}$, $\delta^{34}S_{ts}$, $\delta^{34}S_{ap}$, and $\delta^{34}S_{sas}$). Derived from these calculations, the anthropogenic contribution to the ambient sulfate burden is quantified at 19% during winter and 8% during summer, with these refined values and their accompanying discussions now fully integrated into the revised text.

For more clarity, we have added/revised these sentences as following.

Page 6-7, Lines 167-189 in the revised manuscript:

2.7 Estimation of primary sulfate and secondary sulfate

The underestimation of primary sulfate emissions can partially account for the phenomenon known as missing sulfates. The anthropogenic primary sulfate is estimated as 3% of anthropogenic sources of sulfur emissions in the model. Assuming all the detected concentrations of SO_2 and precursors of secondary sulfate are anthropogenic, we can deduce Eq. (17). Considering the influence of anthropogenic sulfate sources on primary sulfate, the method for estimating primary sulfate can be expressed as follows:

$$n_{ps} = n_{ss} + n_{ts} + n_{ap} \quad (16)$$

$$n_{ap} = 3\% \times \left(n_{SO_2} + n_{sas}\right) \quad (17)$$

$$n_{sas} = n_{tos} - n_{ss} - n_{ts} - n_{ap} \quad (18)$$

where n_{tos}, n_{ps}, and n_{sas} represent the molar concentrations of total, primary, and secondary atmospheric sulfate, respectively, with the primary fraction further resolved into sea-salt (n_{ss}), terrestrial (n_{ts}), and anthropogenic primary (n_{ap}) components. To constrain these natural backgrounds, we employed companion tracer concentrations and mass ratios; specifically, sea-salt sulfate was quantified from soluble Na^+ assuming a purely marine origin (n_{ss}= k[Na^+], where k=[SO_4^{2-}]/[Na^+]=0.25), while terrestrial sulfate was evaluated based on crustal Ca^{2+} abundances (0.18×[Ca^{2+}]). Building upon this physical allocation, the stable sulfur isotope signatures ($\delta^{34}S$) are integrated via an isotopic mass-balance framework to isolate the secondary formation pathways:

$$\delta^{34}S_{obs} = f_{ss} \times \delta^{34}S_{ss} + f_{ts} \times \delta^{34}S_{ts} + f_{ap} \times \delta^{34}S_{ap} + f_{sas} \times \delta^{34}S_{sas} \quad (19)$$

$$f_{ps} = f_{ss} + f_{ts} + f_{ap} \quad (20)$$

Here, $\delta^{34}S_{obs}$ denotes the bulk observed $\delta^{34}S$-SO_4^{2-} value, while the terms prefixed with *f* represent the corresponding molar fractions of each discrete source relative to the total sulfate burden, matched with their respective endmember isotopic signatures where f_{ps}, f_{ss}, f_{ts}, f_{ap}, and f_{sas} are the proportion of primary sulfate, sea salt sulfate, terrestrial sulfate, anthropogenic primary sulfate, and secondary sulfate, respectively ($\delta^{34}S_{ss}$, $\delta^{34}S_{ts}$, $\delta^{34}S_{ap}$, and $\delta^{34}S_{sas}$).

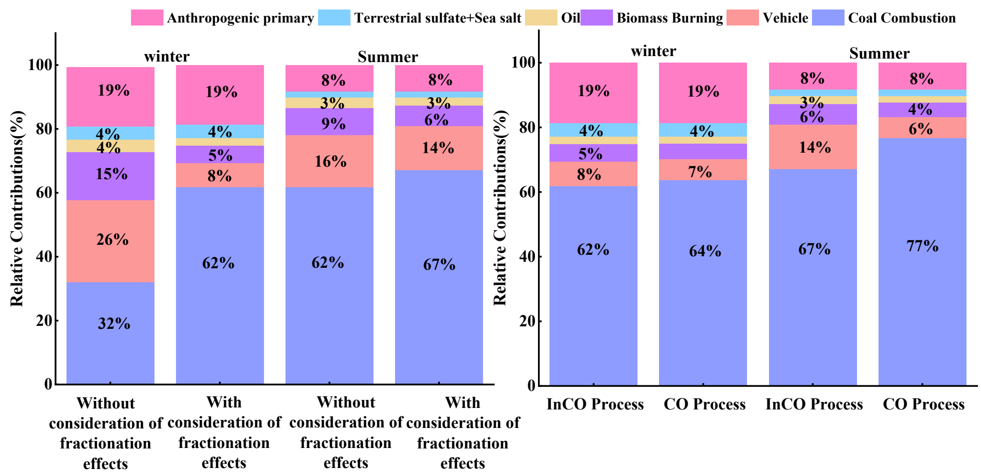

Figure 7. (a) Seasonal variations of source apportionments to sulfate aerosols in Nanjing. (b) Source apportionments of sulfate aerosols in Nanjing resolved by the SIAR model with consideration of fractionation effects under InCO Process and CO Process.

For more clarity, we have added/revised these sentences as following.

Page 16, Lines 293-299 in the revised manuscript:

Neglecting fractionation effects distorts source contributions, yielding winter estimates of 19% (anthropogenic primary sulfate) ,4% (Terrestrial sulfate and Sea salt), 32% (coal), 4% (oil), 15% (biomass), and 26% (vehicle), alongside summer values of 8%, 2%, 62%, 3%, 9%, and 16% (Fig. 7a) respectively-results that inaccurately emphasize traffic emissions contrary to regional emission inventories and chemical transport modeling. Incorporating fractionation factors resolves this discrepancy, aligning sulfate sources with inventory data where coal combustion dominates annually, while idealized complete-oxidation models underestimate summer vehicle contributions by 8% and overestimate coal combustion proportions (about 10%) by comparable margins despite minimal winter deviations.

Reference:

[1] Ding, X., Li, Q., Wu, D., Wang, X., Li, M., Wang, T., Wang, L., and Chen, J.: Direct observation of sulfate explosive growth in wet plumes emitted from typical coalfired stationary sources, Geophys. Res. Lett., 48, e2020GL092071, https://doi.org/10.1029/2020GL092071, 2021.

[2] Alexander, B., Park, R.J., Jacob, D.J., Gong, S., Transition metal-catalyzed oxidation of atmospheric sulfur: global implications for the sulfur budget. J. Geophys. Res. Atmos. 114, D02309, https://doi.org/10.1029/2008JD010486, 2009.

[3] He, P., Alexander, B., Geng, L., Chi, X., Fan, S., Zhan, H., Kang, H., Zheng, G., Cheng, Y., Su, H., Liu, C., and Xie, Z.: Isotopic constraints on heterogeneous sulfate production in Beijing haze, Atmos. Chem. Phys., 18, 5515–5528, https://doi.org/10.5194/acp-18-5515-2018, 2018.

[4] Zheng, M., Song, D., Zhang, D., Cao, Y., and Fan, H.: Using sulfur isotopes to constrain the sources of sulfate in $PM_{2.5}$ during the winter in Jiaozuo City, Atmos. Environ., 332, 120618, https://doi.org/10.1016/j.atmosenv.2024.120618, 2024.

[5] Dasari, S. and Widory, D.: Retrospective isotopic analysis of summertime urban atmospheric sulfate in South Asia using improved source constraints, ACS ES&T Air, 1, 357–364, https://doi.org/10.1021/acsestair.3c00060, 2024.

[6] Dasari, S., Paris, G., Saar, B., Pei, Q., Cong, Z., and Widory, D.: Sulfur isotope anomalies ($\Delta^{33}S$) in urban air pollution linked to mineral-dust-associated sulfate, Environ. Sci. Technol. Lett., 9, 604–610, https://doi.org/10.1021/acs.estlett.2c00312, 2022.

2. Terrigenous sulfate/mineral dust: Please refer to Dasari et al., 2022 ES&T L and 2024 ES&T Air (which should be cited as these are also relevant works to this study) wherein the role of long-range transported mineral dust/terr-sulfate has been shown as an important factor. The authors need to apportion this source, too.

Response: In response to the reviewers' constructive comments, terrigenous sulfate emissions have been rigorously accounted for in our updated budget matrix. The corresponding descriptions in the revised manuscript have been systematically updated to reflect these new calculation results, thereby providing a more accurate representation of localized precursor contributions.

For more clarity, we have added/revised these sentences as following.

Page 16, Lines 286-288 in the revised manuscript:

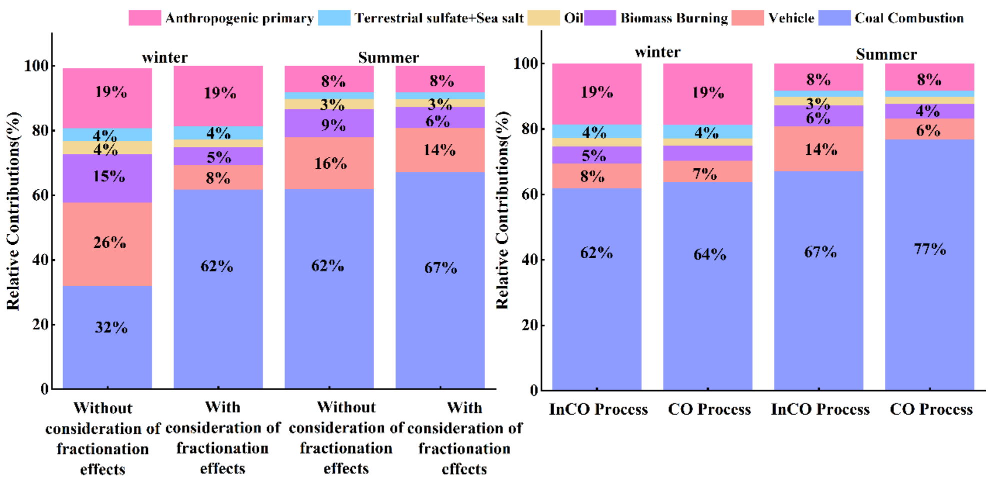

Figure 7. (a) Seasonal variations of source apportionments to sulfate aerosols in Nanjing. (b) Source apportionments of sulfate aerosols in Nanjing resolved by the SIAR model with consideration of fractionation effects under InCO Process and CO Process.

Reference:

[1] Dasari, S., Paris, G., Saar, B., Pei, Q., Cong, Z., and Widory, D.: Sulfur isotope anomalies ($\Delta^{33}S$) in urban air pollution linked to mineral-dust-associated sulfate, Environ. Sci. Technol. Lett., 9, 604–610,

https://doi.org/10.1021/acs.estlett.2c00312, 2022.

[2] Dasari, S. and Widory, D.: Retrospective isotopic analysis of summertime urban atmospheric sulfate in South Asia using improved source constraints, ACS ES&T Air, 1, 357–364, https://doi.org/10.1021/acsestair.3c00060, 2024.

[3] Zheng, M., Song, D., Zhang, D., Cao, Y., and Fan, H.: Using sulfur isotopes to constrain the sources of sulfate in $PM_{2.5}$ during the winter in Jiaozuo City, Atmos. Environ., 332, 120618, https://doi.org/10.1016/j.atmosenv.2024.120618, 2024.

3. Cluster analysis vs. footprint analysis: Please note the AMBTs can show the air masses arriving from a certain region, the footprint of the contributing regions can be very different. Please refer to Dasari et al., 2020 ES&T for this distinction. As such, solely banking on the AMBTs isnt proof enough of the regional source contributions. The authors should convincingly show that the footprint analysis matches the AMBTs.

Response: We sincerely thank the reviewer for highlighting this critical methodological distinction and for directing our attention to the highly relevant work by Dasari et al. (2020). We completely agree with the fundamental premise that while Air Mass Backward Trajectories (AMBTs) effectively delineate atmospheric transport pathways, they do not inherently capture the emission footprint or the actual residence time of pollutants over contributing regions. Consequently, relying exclusively on AMBTs leaves a gap in definitively proving regional source contributions.

To address this insightful critique and comprehensively validate our regional source apportionment, we have significantly expanded our spatial analysis framework. In the revised manuscript, we have introduced rigorous FLEXPART footprint modeling (Figure 4) alongside Concentration Weighted Trajectory (CWT) mapping (Fig. S5). By systematically comparing these advanced diagnostics with our original trajectory clusters (Fig. S4), we can now convincingly demonstrate that the emission footprints perfectly match the AMBTs.

Page 13, Lines 246-249 in the revised manuscript:

Besides, by synergistically combining AMBTs (Fig. S4), CWT (Fig. S5) analysis, and FLEXPART footprint modeling (Fig. 4a, 4b), our integrated framework now successfully bridges the gap between empirical trajectory data and actual emission source strengths. This robust spatial validation explicitly supports our overarching objective to resolve long-standing discrepancies in atmospheric sulfate source attribution.

Page 5-6, in the Supplementary Information:

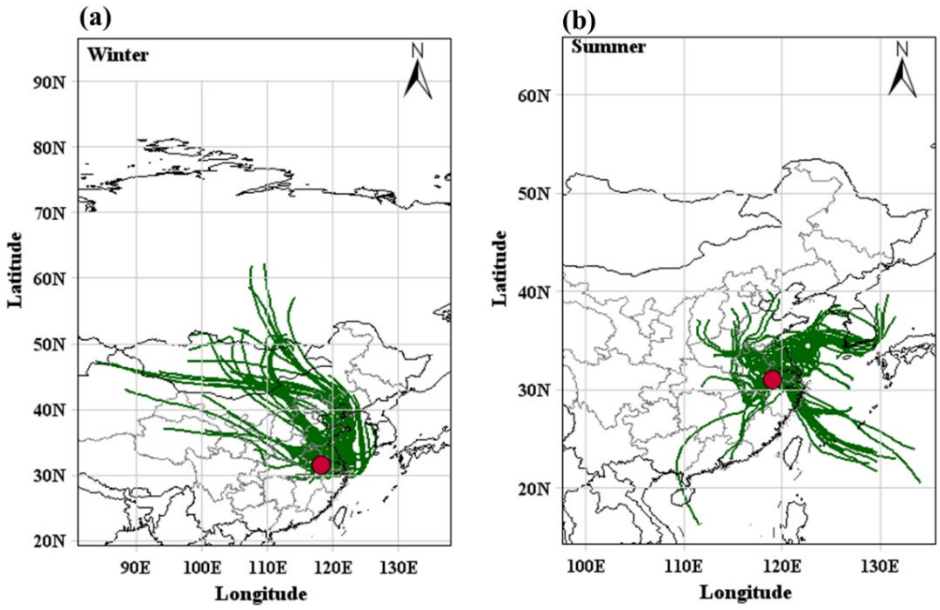

Figure S4. Air mass clusters (a) Winter, (b) Summer.

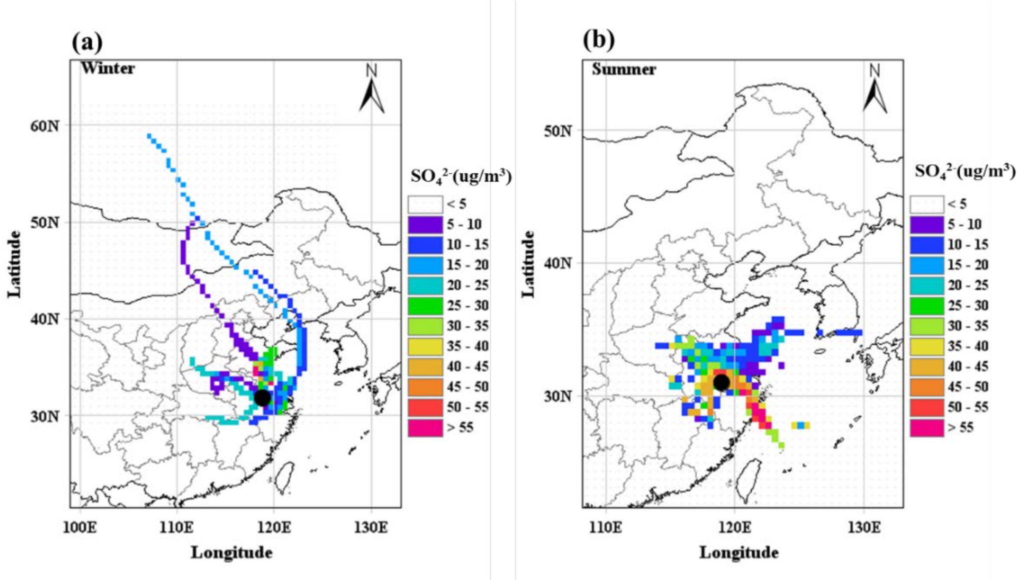

Figure S5. The Concentration weighted trajectory (CWT) maps for sulfate (SO_4^{2-}) mass concentrations ($\mu g\ m^{-3}$) at Nanjing during (a) Winter and (b) Summer are shown, respectively. Color scale represents the SO_4^{2-} mass concentrations.

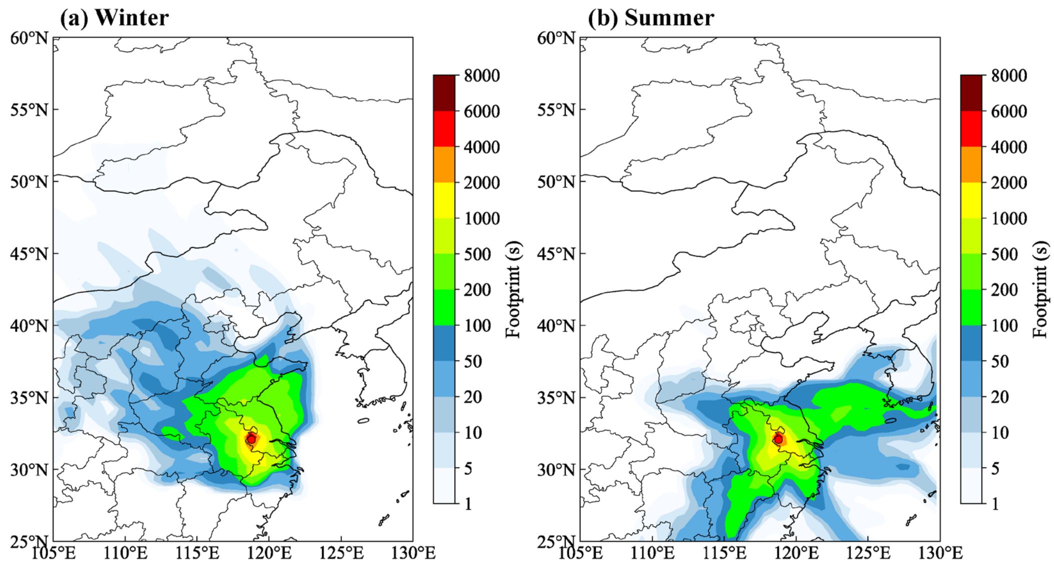

Figure 4. Footprints of sulfate aerosols at the receptor site during the (a) winter and (b) summer computed by the FLEXPART model. The color scale denotes the residence time (s) of sulfate aerosols in the grid cell.

4. NO_2 mediated pathway: Growing evidence suggest this pathway is more active in winter foggy/hazy conditions Wang et al., 2020 Nat. Comm. However, here the authors suggest this pathway is key with contribution in winter and summer nearly the same. This is contradictory to growing body of research (both lab-based and field-based). I suggest the authors reconsider the literature findings and convincingly show this and rethink Fig. 4.

Response: We sincerely appreciate the reviewer for highlighting this critical point and directing our attention to the seminal work by Wang et al. (2020). We completely agree with the growing scientific consensus that the aqueous oxidation of SO_2 mediated by NO_2 is highly sensitive to aerosol liquid water content and pH, making it particularly potent during winter fog and haze conditions. Upon carefully reevaluating our data presentation in Fig 4, we realize that displaying solely the relative percentage contributions inadvertently masked the actual seasonal dynamics of this chemical pathway. While the fractional proportion of the NO_2-mediated pathway appears visually comparable between winter and summer in our isotopic distribution, the absolute mass of sulfate generated via this route differs drastically. Our field measurements demonstrate that total particulate sulfate concentrations peak at 27.55 ± 14.36 μg m^{-3} during severe haze events, which predominantly occur in winter. Consequently, when translating these relative fractions into absolute mass concentrations, the NO_2 pathway produces a substantially higher burden of particulate sulfate in winter compared to summer. This mass-based dynamic aligns perfectly with the enhanced wintertime activity reported by Wang et al. (2020) and the broader field-based consensus. Furthermore, the sustained relative fraction of the NO_2 pathway during the summer months in Nanjing is not an artifact of our isotopic model, but rather a direct reflection of the region's specific emission inventory. As indicated by our $[NO_3^-]/[SO_4^{2-}]$ mass ratio analysis, which yielded values spanning from 0.15 to 1.95, with a mean of 0.98 ± 0.42, mobile vehicular emissions constitute a major atmospheric driver in this region. When these continuous, high-volume NO_x emissions couple with the incomplete SO_2 oxidation regimes characteristic of our summer study site, the NO_2 pathway maintains a significant fractional foothold, even though the absolute sulfate yield remains much lower than in winter. To eliminate this apparent contradiction and integrate the reviewer's excellent insights, we have thoroughly revised the discussion section corresponding to Figure 4 to explicitly distinguish between relative pathway fractions and absolute sulfate mass yields. We formally incorporated Wang et al. (2020) into the text, detailing how our absolute concentration metrics strongly corroborate their lab- and field-based findings regarding enhanced wintertime NO_2 oxidation. We expanded the narrative to clarify how local vehicular NO_x emissions sustain the relative percentage of this pathway during summer, ensuring the isotopic model results are properly contextualized within the region's specific atmospheric chemistry.

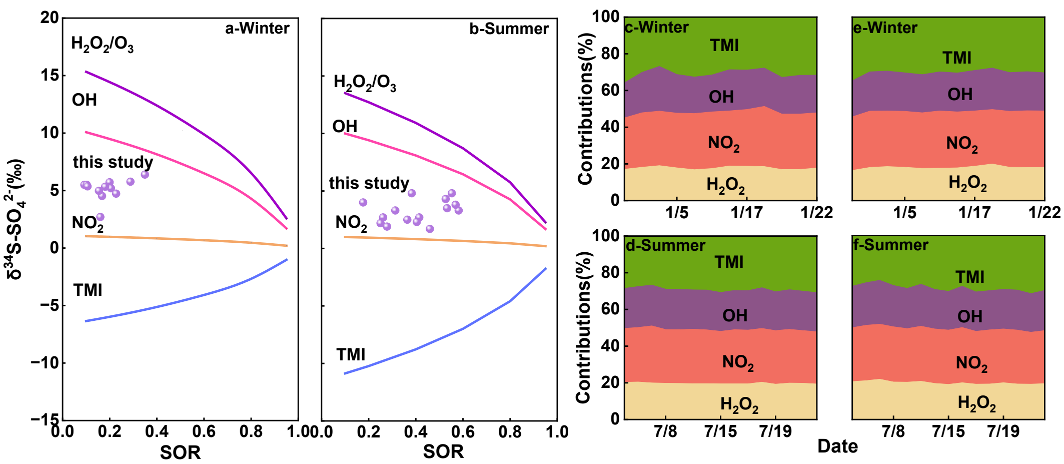

Figure 5. (a, b) Rayleigh fractionation models for secondary SO_4^{2-} formation in

different seasons. (c, d, e, f) Relative contributions of primary, OH, TMI, NO_2, and H_2O_2/O_3 pathways to secondary SO_4^{2-} generation across different seasons. (c, d) represents the fractionation effects under InCO Process; (e, f) represents the fractionation effects under CO Process.

5. Referencing is poor and needs to be updated to correct format and form. Please also add relevant regional works from other parts of the world to address the issue with d34S-based source apportionment of sulfate.

Response: We sincerely appreciate the reviewer's constructive feedback. We have updated and corrected the format and form of the references.

[1] Alexander, B., Park, R. J., Jacob, D. J., and Gong, S.: Transition metal-catalyzed oxidation of atmospheric sulfur: Global implications for the sulfur budget, J. Geophys. Res. Atmos., 114, D02309, https://doi.org/10.1029/2008JD010486, 2009.

[2] Chen, Z., Li, H., Shang, H., Liu, X., Guo, F., Liu, X., Yu, L., Zhou, B., Liu, X., Shi, Y., Zhang, L., and Ai, Z.: Oxalate-promoted SO_2 uptake and oxidation on iron minerals: Implications for secondary sulfate aerosol formation, Environ. Sci. Technol., 57, 13 559–13 568, https://doi.org/10.1021/acs.est.3c03369, 2023.

[3] Dao, X., Lin, Y.., Cao, F., Di, S., Hong, Y., Xing, G., Li, J., Fu, P., and Zhang, Y.: Introduction to the National Aerosol Chemical Composition Monitoring Network of China: Objectives, current status, and outlook, Bull. Amer. Meteorol. Soc.,100, ES337–ES351, https://doi.org/10.1175/BAMS-D-18-0325.1, 2019.

[4] Ding, X., Li, Q., Wu, D., Wang, X., Li, M., Wang, T., Wang, L., and Chen, J.: Direct observation of sulfate explosive growth in wet plumes emitted from typical coalfired stationary sources, Geophys. Res. Lett., 48, e2020GL092071, https://doi.org/10.1029/2020GL092071, 2021.

[5] Guo, Z., Lu, K., Qiu, P., Xu, M., and Guo, Z.: Quantifying SO_2 oxidation pathways to atmospheric sulfate using stable sulfur and oxygen isotopes: laboratory simulation and field observation, Atmos. Chem. Phys., 24, 2195–2205, https://doi.org/10.5194/acp-24-2195-2024, 2024.

[6] Harris, E., Sinha, B., Hoppe, P., and Ono, S.: High-precision measurements of ^{33}S and ^{34}S fractionation during SO_2 oxidation reveal causes of seasonality in SO_2 and

sulfate isotopic composition, Environ. Sci. Technol., 47, 12174–12183, https://doi.org/10.1021/es402824c, 2013a.

[7] He, K., Zhao, Q., Ma, Y., Duan, F., Yang, F., Shi, Z., and Chen, G.: Spatial and seasonal variability of $PM_{2.5}$ acidity at two Chinese megacities: insights into the formation of secondary inorganic aerosols, Atmos. Chem. Phys., 12, 1377–1395, https://doi.org/10.5194/acp-12-1377-2012, 2012.

[8] He, P., Alexander, B., Geng, L., Chi, X., Fan, S., Zhan, H., Kang, H., Zheng, G., Cheng, Y., Su, H., Liu, C., and Xie, Z.: Isotopic constraints on heterogeneous sulfate production in Beijing haze, Atmos. Chem. Phys., 18, 5515–5528, https://doi.org/10.5194/acp-18-5515-2018, 2018.

[9] Lin, M., Zhang, X., Li, M., Xu, Y., Zhang, Z., Tao, J., Su, B., Liu, L., Shen, Y., and Thiemens, M. H.: Five-S-isotope evidence of two distinct mass-independent sulfur isotope effects and implications for the modern and Archean atmospheres, Proc. Natl. Acad. Sci., 115, 8541–8546, https://doi.org/10.1073/pnas.1803420115, 2018.

[10] Lin, Y.-C., Fan, M.-Y., Yu, M., Abulimiti, A., Xie, F., Xu, R., and Zhang, Y.-L.: Significant contributions of regional transport to sulfate aerosols during haze events in northern China Plain: constrained by sulfur isotopic compositions, J. Geophys. Res. Atmos., 130, e2025JD043716, https://doi.org/10.1029/2025JD043716, 2025.

[11] Ma, J., Chen, B., He, Q., Yan, X., Wang, G., Cheng, S., Steil, B., Brühl, C., Pozzer, A., and Lelieveld, J.: Modelling the deep convective transport of trace gases (CO, NH_3 and SO_2) from the planetary boundary layer to the Asian summer monsoon anticyclone, EGUsphere., [preprint], https://doi.org/10.5194/egusphere-2025-5587, 2025.

[12] Mizutani, Y. and Rafter, T.: Oxygen isotopic composition of sulphates. Part 4. Bacterial fractionation of oxygen isotopes in the reduction of sulphate and in the oxidation of sulphur, N. Z. J. Sci., 12: 60-8, https://www.osti.gov/biblio/4764537, 1969.

[13] Mukai, H., Tanaka, A., Fujii, T., Zeng, Y., Hong, Y., Tang, J., Guo, S., Xue, H., Sun, Z., Zhou, J., Xue, D., Zhao, J., Zhai, G., Gu, J., and Zhai, P.: Regional characteristics of sulfur and lead isotope ratios in the atmosphere at several Chinese urban sites,

Environ. Sci. Technol., 35, 1064–1071, https://doi.org/10.1021/es001399u, 2001

[14] Ruan, X., Zhao, C., Zhou, T., Zhang, Z., Ma, T., Wang, X., Zhao, W., Su, G., and Geng, L.: Cloud and aerosol chemistry together explain the high sulfate aerosol content in a heavy haze episode in Central Eastern China, Environ. Sci. Technol., 59, 23398–23409, https://doi.org/10.1021/acs.est.5c07415, 2025.

[15] Tanaka, N., Rye, D. M., Xiao, Y., and Lasaga, A. C.: Use of stable sulfur isotope systematics for evaluating oxidation reaction pathways and in-cloud-scavenging of sulfur dioxide in the atmosphere, Geophys. Res. Lett., 21, 1519–1522, https://doi.org/10.1029/94GL00893, 1994.

[16] Tao, Y., Ye, X., Ma, Z., Xie, Y., Wang, R., Chen, J., Yang, X., and Jiang, S.: Insights into different nitrate formation mechanisms from seasonal variations of secondary inorganic aerosols in Shanghai, Atmos. Environ., 145, 1–9, https://doi.org/10.1016/j.atmosenv.2016.09.012, 2016.

[17] Wang, W., Yu, J., Cui, Y., He, J., Xue, P., Cao, W., Ying, H., Gao, W., Yan, Y., Hu, B., Xin, J., Wang, L., Liu, Z., Sun, Y., Ji, D., and Wang, Y.: Characteristics of fine particulate matter and its sources in an industrialized coastal city, Ningbo, Yangtze River Delta, China, Atmos. Res., 203, 105–117, https://doi.org/10.1016/j.atmosres.2017.11.033, 2018.

[18] Yanagisawa, F. and Sakai, H.: Thermal decomposition of barium sulfate-vanadium pentoxide-silica glass mixtures for preparation of sulfur dioxide in sulfur isotope ratio measurements, Anal. Chem., 55, 985–987, https://doi.org/10.1021/ac00257a046, 1983.

[19] Yu, C., Liu, T., Chi, X., Huang, X., and Ding, A.: Salting-in of HCHO sustains fast hydroxymethanesulfonate formation in deliquesced sulfate aerosols, Environ. Sci. Technol. Lett., 13, 744–750, https://doi.org/10.1021/acs.estlett.6c00300, 2026.

[20] Zhang, R. and Chan, C. K.: Simultaneous formation of sulfate and nitrate via co-uptake of SO_2 and NO_2 by aqueous NaCl droplets: combined effect of nitrate photolysis and chlorine chemistry, EGUsphere [preprint], https://doi.org/10.5194/egusphere-2023-223, 2023.

[21] Zhang, X., Liu, J., Li, H., Zuo, Y., Zhang, C., Su, Z., Wang, S., Zhang, P., Chu, B.,

and He, H.: pH-dependent Fe(III) speciation and concerted proton–electron transfer mechanism accelerated S(IV) oxidation at the air–water interface, J. Am. Chem. Soc., 148, 11812–11821, https://doi.org/10.1021/jacs.5c21077, 2026.

6. While the study is interesting, there are many caveats (e.g, with pathway attribution) as such some wording like 'paradigm shift' seem unncessary. I suggest the authors to reconsider such wordings.

Response: We are deeply grateful for the reviewer's constructive feedback, which has prompted a comprehensive linguistic refinement of the entire manuscript to ensure maximum clarity and scientific readability.